JIPK. Volume 17 No 2 June 2025
Sinta 1 (Decree No: 158/E/KPT/2021)
e-ISSN:2528-0759; p-ISSN:2085-5842
Available online at https://e-journal.unair.ac.id/JIPK

JIPK
(JURNAL ILMIAH PERIKANAN DAN KELAUTAN)
Scientific Journal of Fisheries and Marine

Research Article

Water Mass and Indirect Estimation of Turbulent Mixing Based on Observational CTD Yoyo Data in Flores Sea Waters, Indonesia

Gentio Harsono[1,2*], Amir Yarkhasy Yuliardi[3], Anindya Wirasatriya[4], Budi Purwanto[2], and Mario Cabral[5]

[1]Faculty of Science and Defense Technology, Republic Indonesia Defense University, Bogor. Indonesia
[2]Hydro-Oceanography Center, Indonesian Navy, Jakarta. Indonesia
[3]Department of Marine Science, Faculty of Fisheries and Marine Science, Jenderal Soedirman University, Purwokerto. Indonesia
[4]Department of Oceanography, Faculty of Fisheries and Marine Science, Diponegoro University, Semarang. Indonesia
[5]Department of Marine Science and Fisheries, Universidade Nacional Timor Lorosa'e. Timor-Leste

OPEN ACCESS

ARTICLE INFO

Received: March 12, 2025
Accepted: April 30, 2025
Published: May 08, 2025
Available online: May 25, 2025

*) Corresponding author:
E-mail: hgentio1969@gmail.com

Keywords:
Water Mass
Turbulent mixing
Mixing CTD
Yoyo method
Flores Sea

Abstract

The Flores Sea is on the western ITF trajectory connecting the Pacific and Indian oceans. Identification and quantification of turbulent mixing of water masses in the Flores Sea are essential for analyzing large-scale ocean circulation processes, including the circulation of the Indonesian ocean interior. However, direct estimations of turbulent mixing in the Flores Sea as a part of the ITF are underestimated. This research aims to determine water conditions, stratification, and water mass structures. This research used data obtained from the CTD instrument applying a Yoyo casting method deployed in March − April 2023. On the other hand, the Thorpe method was used to estimate turbulent vertical mixing based on the values of energy dissipation and vertical diffusivity. The waters are stratified into three layers, mixed layer (1−50 m), thermocline layer (50−180 m), and deep layer (180−500 m). The CTD data showed the presence of a stable thermocline layer dominated by ITF water masses carrying water masses from the Pacific Ocean (North Pacific Intermediate Water (NPIW) and North Pacific Subtropical Water (NPSW)) from the western ITF path. The energy dissipation value obtained at the study site was about 3.36E-07 W Kg-1 and the vertical diffusivity value was approximately 5.25E-05 m2s-1. The thermocline layer showed a large energy dissipation value which was strongly associated with the friction of the ITF, suggesting that turbulent mixing in this region is primarily driven by the interaction of ITF water masses with the surrounding environment.

Cite this as: Harsono, G., Yuliardi, A.Y., Wirasatriya, A., Purwanto, B., & Cabral, M. (2025). Water Mass and Indirect Estimation of Turbulent Mixing Based on Observational CTD Yoyo Data in Flores Sea Waters, Indonesia. *Jurnal Ilmiah Perikanan dan Kelautan,* 17(2):358-373. https://doi.org/10.20473/jipk.v17i2.70809

1. Introduction

Turbulent mixing processes play a significant role in amplifying the vertical transport of heat, maintaining ocean stratification, and driving global currents (Wunsch and Ferrari, 2004). In addition, at the exposure level, turbulent mixing also affects the redistribution of nutrients, pollutants, sediments and freshwater to the water column (Sharples *et al.,* 2001). Ocean dynamics and climate variability are first-order governed by turbulent mixing processes that can currently only be resolved by means of parameterizations, typically in vertical diffusivity (Fox-Kemper *et al.,* 2019). Several studies have focused on improving the parameterization with respect to local flow characteristics (Gregg *et al.,* 2018; Caulfield, 2021). The primary generating sources of ocean mixing in the surface layer are driven by wind stress and buoyancy fluxes (Liu *et al.,* 2022), while in the water column, it is controlled by inertial motion forces and external/internal tidal propagation (Purwandana *et al.,* 2020; Nagai *et al.,* 2021).

The Indonesian Archipelago is the only low-latitude link between the Pacific and Indian oceans, passing through rough bathymetry and narrow gaps, known as the Indonesian Throughflow (ITF) (Sprintall *et al.,* 2004; Nagai and Hibiya, 2015). On a time scale, its variation is intraseasonal to annual, and it is influenced by the difference in sea level of the Pacific Ocean and Indian Ocean (Wyrtki, 1961; Susanto and Song, 2015; Sprintall *et al.,* 2019). This region has many tidal mixing points as an interaction between flow and rough bathymetry, which is cited as one of the factors in changing the physical properties of seawater (Koch-Larrouy *et al.,* 2010; Sprintall *et al.,* 2014; Nagai and Hibiya, 2020; Purwandana *et al.,* 2020; Nagai *et al.,* 2021). Explicitly, Ray and Susanto (2016) found the influence of tidal mixing on SST changes in the tidal cycle which is clearly visible in SST data using satellite observations. Therefore, Indonesian waters play an important role in climate regulation through changes in temperature and salinity in the Pacific and Indian Oceans that impact the dynamics of the monsoon system, the El Niño Southern Oscillation (ENSO) walker circulation and the Indian Ocean Dipole (IOD) (Sprintall *et al.,* 2019).

The Flores Sea is on the western ITF trajectory that connects the Pacific and Indian oceans. The western ITF transports water masses from the North Pacific that enter Indonesian waters through the Sulawesi Sea, Makassar Strait, Flores Sea and some go directly to the Indian Ocean through the Lombok Strait (Atmadipoera *et al.,* 2009; Sprintall *et al.,* 2019) and it is identified as the North Pacific Intermediate Water (NPIW) and North Pacific Subtropical Water (NPSW) water masses characterized water masses through the western ITF route (Silaban *et al.,* 2021). In addition to the western ITF water mass, the Flores Sea is also influenced by the eastern ITF recirculation in the northwest part of Banda. The Flores Sea is indicated to be influenced by intra-seasonal, semi-annual, annual and inter-annual variability at work (Putriani *et al.,* 2019). The ITF water mass entering Indonesian waters not only changes the temperature value which then becomes a climate regulator, but also affects the habitat of biota in the Flores Sea (Putri *et al.,* 2021). The Flores Sea also receives the influence of internal waves that propagate from the place of generation in the Sape Strait as observed from satellite imagery (Karang *et al.,* 2019). Many phenomena and ocean variability that occur in the Flores Sea make these waters quite complex and interesting to study.

Identifying and quantifying the turbulent mixing of water masses in the Flores Sea is essential for analyzing large-scale ocean circulation processes and the circulation of the Indonesian ocean interior. However, direct measurements have never been carried out to estimate turbulent mixing in the Flores Sea, specifically at the research site, and the estimated value is not known with certainty. Field measurements conducted by the Indonesian Navy Hydrography and Oceanography Center (PUSHIDROSAL) in the waters of the Flores Sea as part of the Jala Citra 3 Flores Expedition aimed to understand and reveal the oceanographic conditions in the Flores Sea to complement the data and knowledge with respect to Indonesian waters. We attempted to use the newly acquired data in the expedition to fill the gaps in oceanographic data measurements from previous ITF-related studies. This study aims to describe the general condition of the water, stratification and water mass structure in the Flores Sea, and estimate the dissipation coefficient and vertical diffusivity of turbulent mixing using the Thorpe Method acquired from the CTD instrument with "Yoyo" measurements. We describe herein our findings about the physical dynamics of waters in the Flores Sea, the transformation and identification of ITF water masses, and the value of turbulent mixing from indirect measurements.

2. Materials and Methods

2.1 Materials

2.1.1 The equipments

We measured the depth, temperature, salinity and sound velocity profiles using the MIDAS SVX2 CTD instrument package with the ship-derived Yoyo casting method. The MIDAS SVX2 CTD has a sam-

pling rate of 8 Hz and a sampling period of 8 secs with a measurement interval time of 0.125 secs. The observation point is on the westbound ITF line (Atmadipoera *et al.,* 2009; Sprintall *et al.,* 2019) which is passed by internal wave (tidal) propagation that has previously been observed (Karang *et al.,* 2019), that internal tides with large amplitudes are thought due to the interaction between tides and strong topography (Nagai and Hibiya, 2015).

The location of observation with initial coordinates 122.3868° East and -6.5177° South and during low tidal conditions according to the measurement data at the Baubau tide station (the closest station to the CTD data collection location) (Figure 1B, 1C). 9 profiles, with depths approximately ~500 m, were acquired between 22:02 local time on 26-Apr-23 and 05:58 local time on 27-Apr-23 (Figure 1D).

Tidal data at Baubau station was provided by the Geospatial Information Agency (BIG), accessed on 26-27 Mar-2023, webpage http://srgi.big.go.id/tides/with a measurement interval of 1 min. Meteorological conditions during the observation period were estimated using datasets retrieved from the European Center for Medium-Range Weather Forecasts (ECMWF) reanalysis 5 (ERA-5). Wind parameters were obtained from https://cds.climate.copernicus.eu/ with spatial and temporal resolution of 0.25° × 0.25° and 1 h, respectively (Hersbach *et al.,* 2023). We displayed wind speed and direction data at locations and times that coincided with Yoyo CTD data. For current conditions, we used weekly near-real-time (NRT) data assimilated from *in situ* and satellite data (ARMOR3D) that can be accessed at https://data.marine.copernicus.eu/ with a temporal resolution of 0.25° × 0.25° and available up

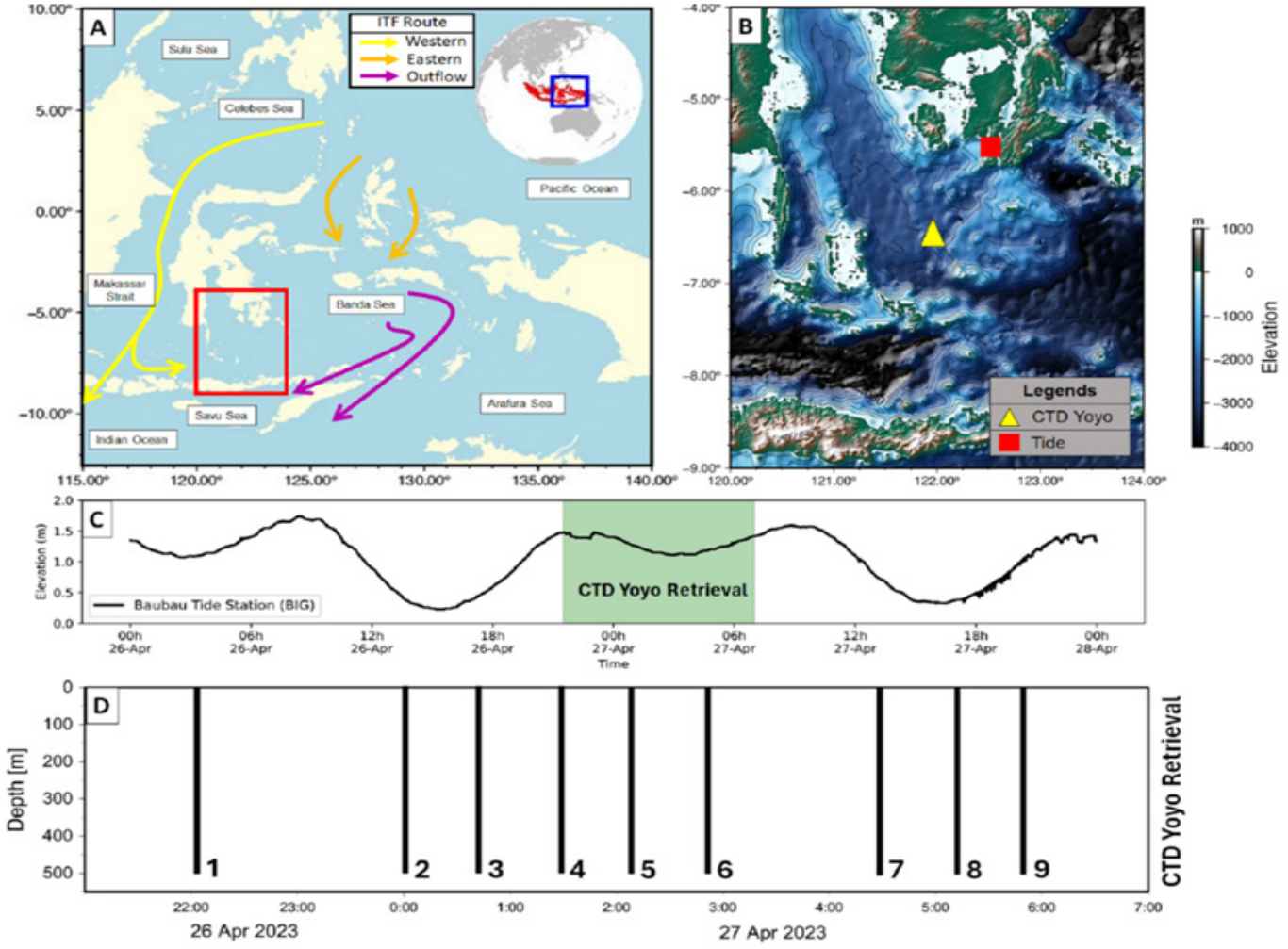

Figure 1. (A) Indonesian transboundary currents westward (yellow line), eastward (orange line) and outward (purple line) (Sprintall *et al.,* 2009; Gordon *et al.,* 2010; Susanto *et al.,* 2015) with red box highlighting the study area. (B) The study site is in the Flores Sea region, yellow triangle of Yoyo CTD collection site and red box of Baubau tidal station with bathymetry contours. (C) Tidal conditions at the time of CTD Yoyo data collection based on the nearest tidal observation station (Baubau). (D) CTD Yoyo data collection for 9 replicates between 22:00 and 06:00 local time.

to 50 depth levels (Guinehut *et al.*, 2012; Mulet *et al.*, 2012). We chose 3 depth levels to observe current direction and velocity: surface layer data for the mixed layer, 125 m depth for the thermocline layer, and 450 m depth for the deep layer.

2.1.2 The materials

Direct field observations were conducted using KRI Spica-934 provided by the Indonesian Navy Hydrography and Oceanography Center (PUSHIDROSAL) in the framework of the Jala Citra 3 Flores Expedition, focused on the Flores Sea as one of main routes of the western ITF (Figure 1A). The expedition was divided into 4 stages to collect oceanographic, meteorological, geological and biological data during the period of March to April 2023. The observations were divided into several CTD drop points based on predetermined stages.

2.1.3 Ethical approval

This study does not require ethical approval because it does not use experimental animals.

2.2 Methods

The field data was evaluated to determine the hydrographic structure, general characteristics and stratification of water masses at the study site on April 26-27, 2023. The data acquired from the CTD were extracted, calculated and plotted. Water mass stratification was analyzed using the calculation of temperature gradient changes to identify the thickness of the thermocline layer in the water marked by the upper and lower boundaries of the thermocline layer. The determination of the water mass layer is based on the temperature gradient, where the temperature gradient value of the thermocline layer is more than or equal to 0.05 C/m (Hao *et al.*, 2012). The structure of the water mass during observation using the Yoyo CTD will be described or identified. By analyzing the values of temperature and salinity associated with a particular water mass, the type of water mass in a water body using the Temperature-Salinity (TS) diagram (Emery, 2001) could be estimated. Water mass types have their own characteristics. Data was collected during the transitional monsoon so that the influence was not as strong as during the east monsoon.

2.3 Analysis Data

The vertical stability structure of the water mass was identified based on the Brunt-Väisälä and Thorpe displacement values identified from the 9 replicates of the Yoyo CTD. The diapycnal (turbulent) mixing that occurs can be measured based on the results of temperature and salinity profile measurements (Ferron *et al.*, 1998; Yang *et al.*, 2014). In this study, the estimation of turbulent mixing based on density reversal occurred using the method introduced by Thorpe (1977) and further developed by Dillon (1982). Calculation of potential density ($\rho\theta$) at each temperature and salinity profile from the Midas SVX2 "Yoyo" CTD instrument using the Gibbs-Sea-Water (GSW) Oceanographic Toolbox (McDougall and Barker, 2011). Potential density is a variable that does not include density variations due to compressibility (Jackett and McDougall, 1995), hereafter defined as density. Meanwhile, the background buoyancy frequency or frequency Brunt-Väisälä (N^2) with limitation is estimated based on one-dimensional profile sorting (Arthur *et al.*, 2017). Each density profile will be sorted in a stable (gravity) configuration with the measured density to see any density inversion as the Thorpe length scale (LT) (Thorpe, 1977; Dillon, 1982). The Thorpe scale (LT) value is defined as the RMS value for each turbulent patch d_i:

$$L_T = (1/n \sum_{i=1}^{n} Td^2_i)(1/2) \quad \text{.....(i)}$$

Where:

n = the total number of data points or samples

Td^2_i = the temperature deviation at point,

i = the difference between the actual temperature and

a reference or mean temperature.

Thorpe (1977) stated that the estimated length of the turbulent scale is associated with the occurrence of a water mass reversal and the water mass reversal has a close relationship with the Ozmidov scale. The relationship between the Ozmidov scale has been written in the equation:

$$L_o = (\varepsilon/N^3)(1/2) \quad \text{.....(ii)}$$

Where:

L_o = the characteristic length scale associated with turbulence

ε = the rate of turbulent kinetic energy dissipation

N = the buoyancy frequency,

which describes the stability of stratified fluids. Estimation of kinetic energy dissipation value by entering calculation components according to the equation:

$$\varepsilon = L^2_o \, N^3 \quad \text{.....(iii)}$$

The results of the energy dissipation calculation are entered into the equation:

$K_z = \gamma\varepsilon / N^2$.....(iv)

Where:

K_z = the vertical eddy diffusivity, which quantifies the mixing efficiency in a stratified fluid.

γ = is the mixing efficiency coefficient, typically determined empirically, the mixing efficiency (γ) value used is 0.2 as stated by Osborn (1980) and Purwandana *et al.* (2020).

3. Results and Discussion

3.1 Results

3.1.1 General conditions

The tidal system in Indonesian waters is tremendously complex. It is generated by the interactions between bathymetry profile, coastline variation, and mixing of tidal wave propagation from the Pacific and Indian Oceans. This intricate interaction leads to unique tidal elevations, currents, and energy flux patterns in the impacted region (Wei *et al.,* 2016). Tides can be predicted based on the amplitude and phase lag values of their harmonic components, which are represented by co-phase and co-range. In Indonesian waters, the co-phase and co-range indicate that the M2 semidiurnal tidal component is primarily influenced by the Indian Ocean. In contrast, the K1 diurnal tidal component moves in the opposite direction to the M2 semidiurnal tide (Ray *et al.,* 2005). Reaching the Banda Sea and Flores Sea, a collision of two tidal waves takes place, resulting in increased amplitude in the Flores Sea, then moves westward to the Java Sea (Ray *et al.,* 2005). In this study, a double daily inclined mixed tide type was clearly identified based on direct observation data at the Baubau tidal station (Figure 2A). Similar results were obtained by Atmaja *et al.* (2019) based on a model with the dominant M2 tidal component and meridional tidal currents (north south direction).

Wind movement patterns in Indonesia generally follow the movement of the monsoons. The wind moves in different directions in each monsoon. In this study, the data was collected in April 2023, which is within the phase of the first transitional monsoon, strongly influenced by winds from Australia to Asia with the primary directions to the southwest/northwest with a speed range of 1.4–4.7 m/s (Figure 2B, 2C). In the MAM-JJA phase, winds from the southeast (Australia) began to blow quite stably and gradually increased wind speed and began to align with the coastline on the southern island of Sulawesi (Habibi *et al.,* 2012). As a result of the southeast wind parallel to the coastline and the Coriolis force, the southern part of Sulawesi and the northern part of the Flores Sea have been identified as the upwelling zone (Kunarso *et al.,* 2018; Kurniawan *et al.,* 2018; Napitupulu *et al.,* 2022) where the transport of water masses away from the coast is the most significant factor in this event (Atmadipoera and Widyastuti, 2014).

The current flow in each layer is determined by its speed and direction. The vector overlay of current direction and velocity (water mass circulation) during the study at the depth of the surface layer, 125 m depth and 450 m depth is described in Figure 3. In each layer, the direction moves towards the east with the highest velocity in the surface layer of about 0.64 m/s and successively decreases with increasing depth; at the 125 m depth, it reaches 0.45 m/s and at the 450 m depth, it peaks at 0.40 m/s. The eastward propagation of currents from the eastern Java Sea to the Flores Sea continues to the Banda Sea occurs from November to May (Atmadipoera *et al.,* 2009) and this circulation is mainly influenced by surface winds. During the westerly monsoon, the eastern ITF disappears and is driven by water from the Java Sea and the eastern ITF reappears during the easterly monsoon (Du and Qu, 2010). The current speed of the western ITF is usually stronger during the eastern monsoon (July to September) with a maximum speed of -0.8 m/s near 120 m and decreases during the western monsoon transition (Atmadipoera and Widyastuti, 2014).

3.1.2 Hydrological structure

The vertical profiles of temperature, salinity and density parameters are presented in Figure 4. The thermocline layer was identified at a depth of 50–180 m with a thickness of 130 m (Figure 4A). In the thermocline layer, there are traces of water masses characterized by maximum salinity with values close to 35 psu (Figure 4B). The density profile shows a gradient that aligns with temperature, indicating a close relationship between temperature and density (Figure 4C). Temperature is a factor that significantly affects water delamination followed by salinity (Liu *et al.,* 2016). Based on the observation of temperature against depth, three layers are well-observed, which will be used to analyze the mixing in each layer.

To see the transverse distribution of water mass at the study site based on the time of Yoyo CTD collection, a cross-sectional structure of the oceanographic parameters (temperature, salinity and density) is made, shown in (Figure 5). The water stratification is well-observed, consisting of homogeneous layers, thermocline layers and deep layers. The surface layer shows minimal or relatively uniform changes in temperature (> 29.5°C), salinity (< 33.5 psu), and density

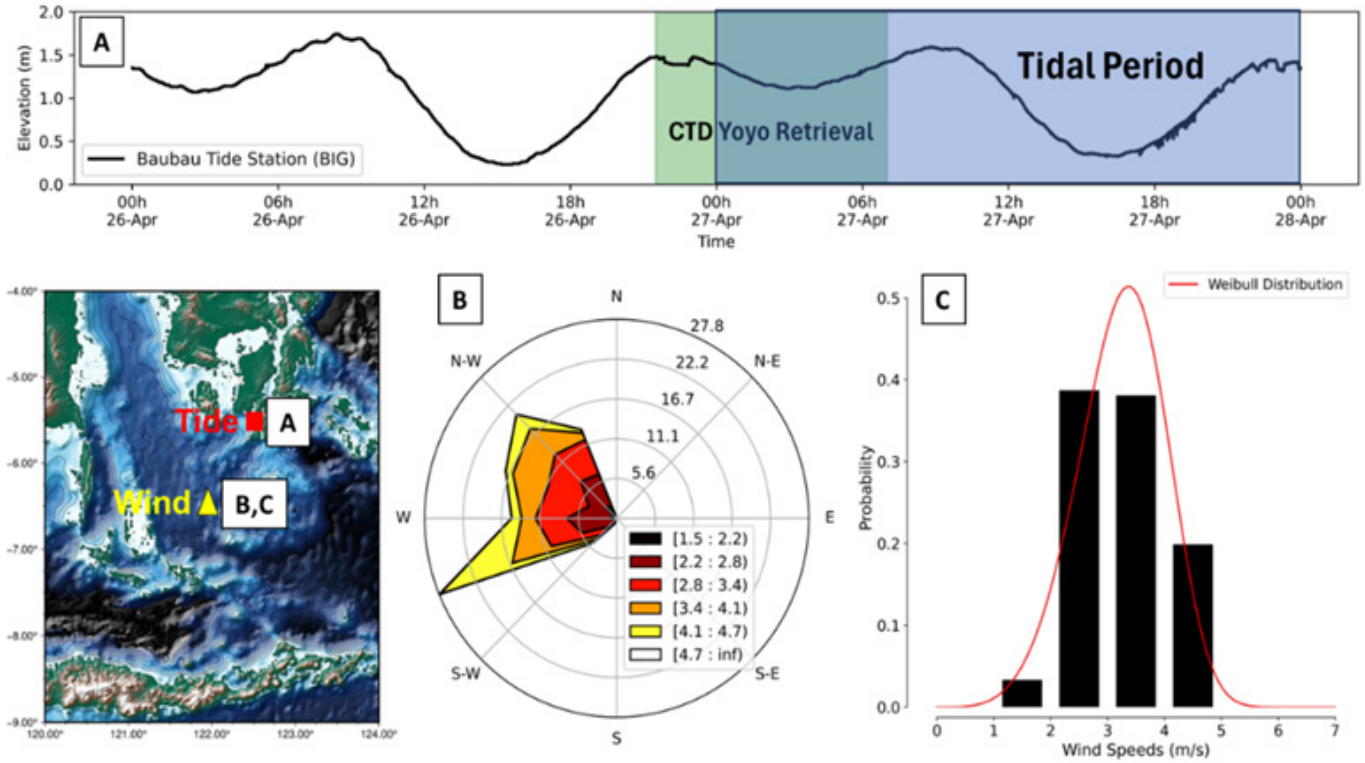

Figure 2. (A) Tidal period at Baubau observation station. (B) Windrose showing wind direction and speed and (C) Histogram of wind speed at CTD Yoyo observation point.

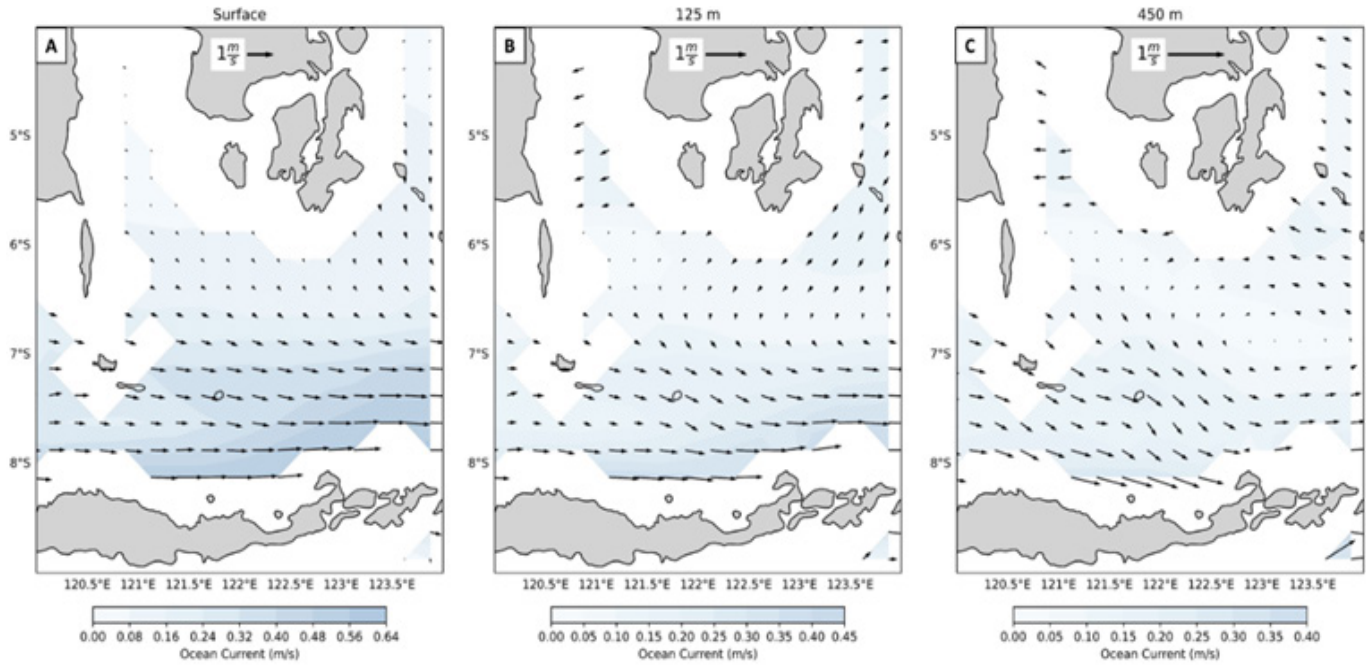

Figure 3. Spatial distribution of ocean currents at (A) Surface layer depth, (B) 125 m depth and (C) 450 m depth during the deployment of Yoyo CTD. Scale bar and current velocity vector (1 m/s) for each figure.

(< 21 kg/m³). This layer starts from the surface layer to a depth range of 50 m. The thermocline layer was identified in the depth range of 50–180 m. The isothermal and isopycnic lines are clearly visible due to significant changes in values. The temperature parameter shows traces of water masses characterized by high salinity up to the study site. This water mass is identified with water masses from the Pacific Ocean that

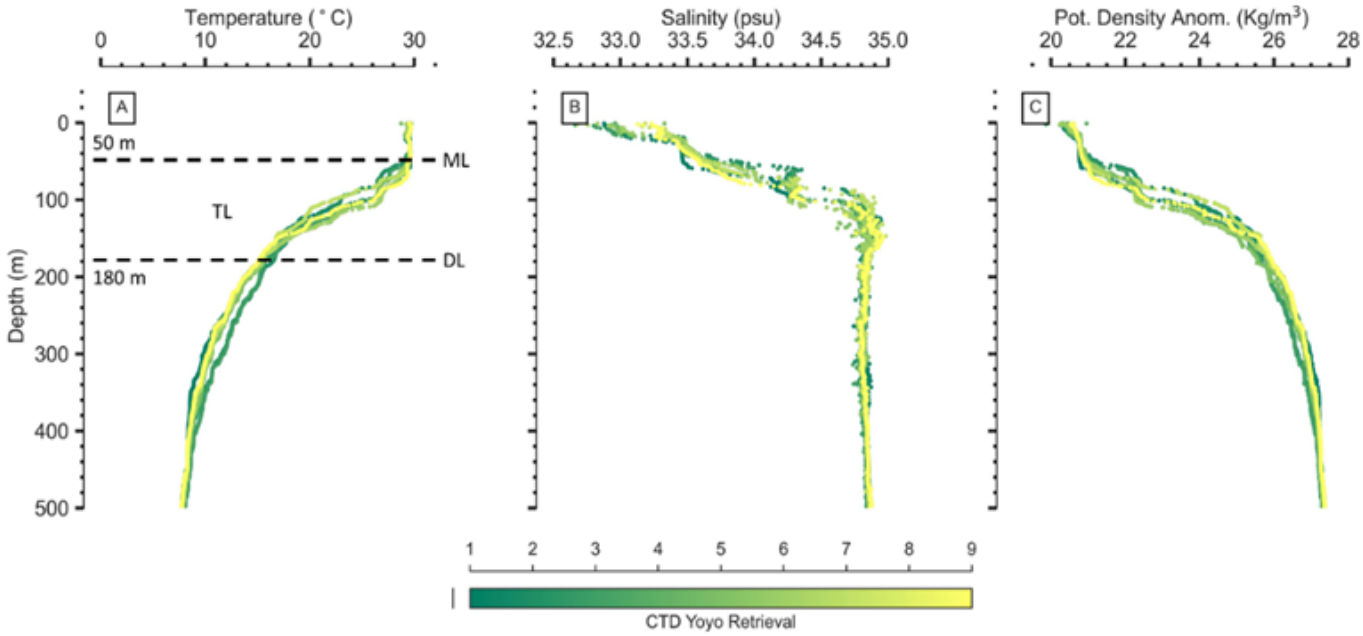

Figure 4. Vertical profiles of (A) Temperature with description of mixed layer (ML), thermocline layer (TL), deep layer (DL), (B) Salinity and (C) Density. Color gradations indicate CTD replicates.

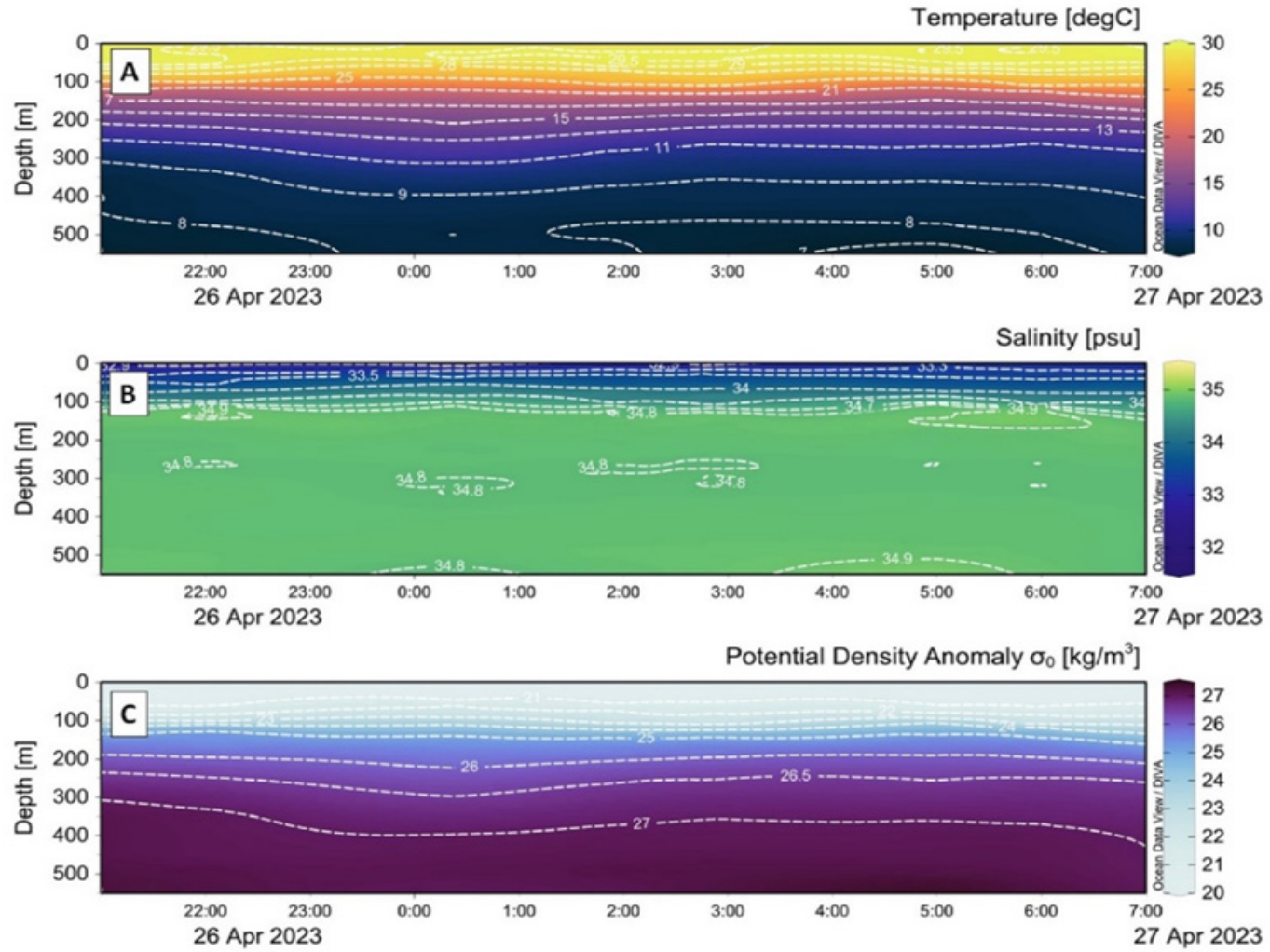

Figure 5. Cross-sectional profiles against depth during the CTD Yoyo data collection period (A) Temperature (B), Salinity and (C) Density in sequence.

enter Indonesian waters through the ITF (Atmadipoera *et al.,* 2009; Sprintall *et al.,* 2019; Purwandana *et al.,* 2020). After reaching a depth of 180 m (deep layer) the vertical gradient of temperature and density is quite weak and tends to be homogeneous again. Meanwhile, the salinity parameter decreases with depth until the minimum salinity point and then becomes more homogeneous. The density value appears to have a similar gradient with temperature because in offshore or open waters the density value is more significantly influenced by temperature (Liu *et al.,* 2016).

After considering and reviewing the world water mass classification (Emery, 2001), this study identified 4 types of water masses (Figure 6). The first one is the Java Sea Water (JSW), identified at a depth of 0–23 m with temperature and salinity ranging from 29.1–29.7 ˚C and 32.2–33.4 psu, respectively (Figure 6B). It is in the surface layer dominated by water masses with low salinity characteristics (fresh) which is associated with a strong influence from the Java Sea (Gordon *et al.,* 2010; Susanto *et al.,* 2012). The second water mass is water column between the surface and the ITF water masses, with temperature ranging from 36.5–29.4˚C and salinity of 33.6–34.4 psu at a depth of 53 - 87 m (Figure 6C). This water mass was also previously identified in the Lombok Strait (Yuliardi *et al.,* 2021) and Bali Sea (Harsono *et al.,* 2021), which also aligns with the ITF of the Flores Sea from the Makassar Strait (Fan *et al.,* 2018). The third water mass, the NPSW water mass at 105–172 m depth, is characterized by a temperature of 15.7–23.8˚C and salinity of 34.5–35 psu (Figure 6D). The fourth water mass is the NPIW water mass at a depth of 248–343 m, characterized by a temperature of 9.6–13˚C and salinity of 34.6–34.8 psu (Figure 6E). The third and fourth water masses belong to ITF water masses. The NPSW (NPIW) water mass is characterized by maximum (minimum) salinity originating from the northern Pacific Ocean which enters the Indonesian waters through the ITF (Atmadipoera *et al.,* 2009; Sprintall *et al.,* 2019; Purwandana *et al.,* 2020).

3.1.3 Turbulent mixing

The vertical water mass stability structure is identified based on the Brunt Vaisala value and Thorpe displacement identified from 9 CTD Yoyo repetitions which can be seen in (Figure 7). The relationship between the Brunt Vaisala frequency and Thorpe displacement is clear enough to describe the stability of the water mass in a body of water. In general, all repetitions show the same/quite similar pattern. The

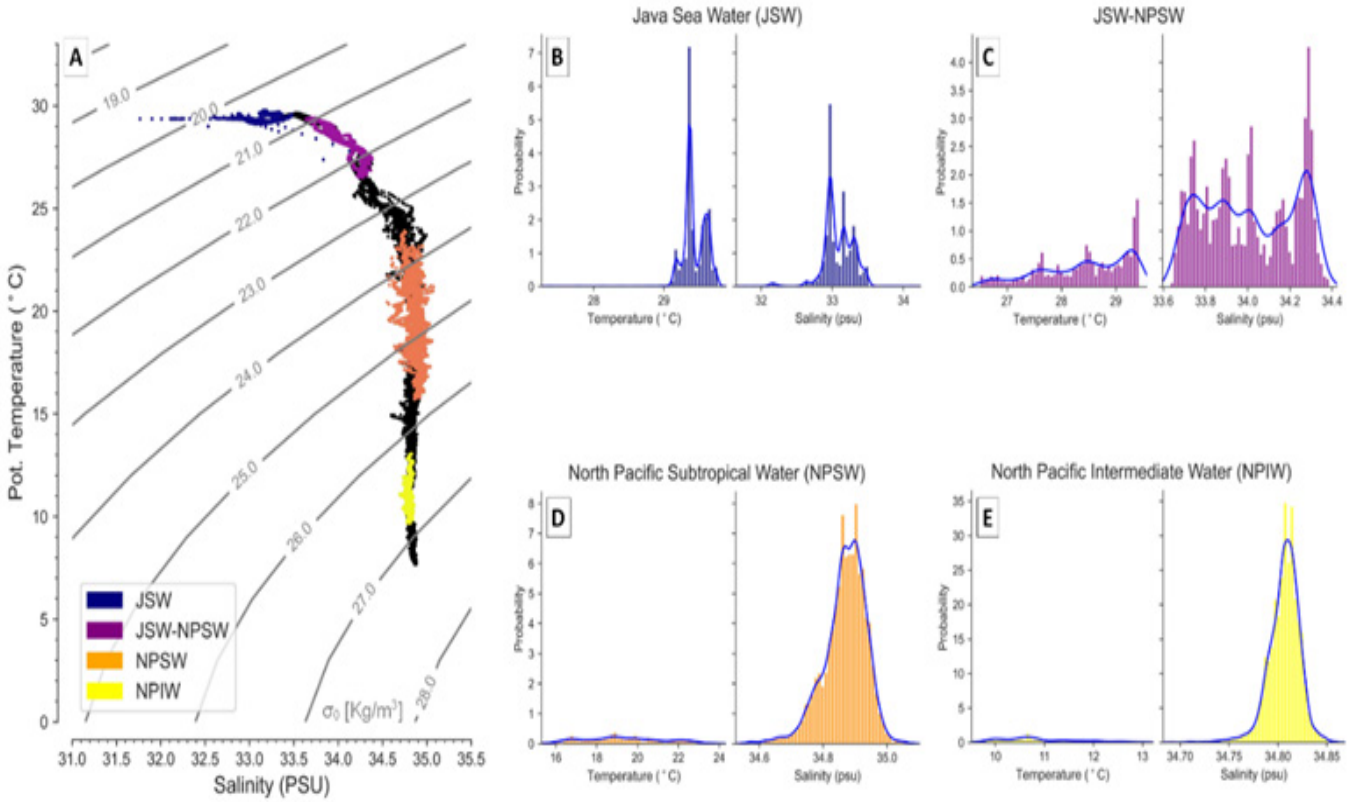

Figure 6. (A) T-S diagram with different water mass types with different colors, JSW (navy), JSW-NPSW (purple), NPSW (orange) and NPIW (yellow). Probability diagram of temperature and salinity in water mass types (B) JSW, (C) JSW-NPSW, (D) NPSW and (E) NPIW respectively.

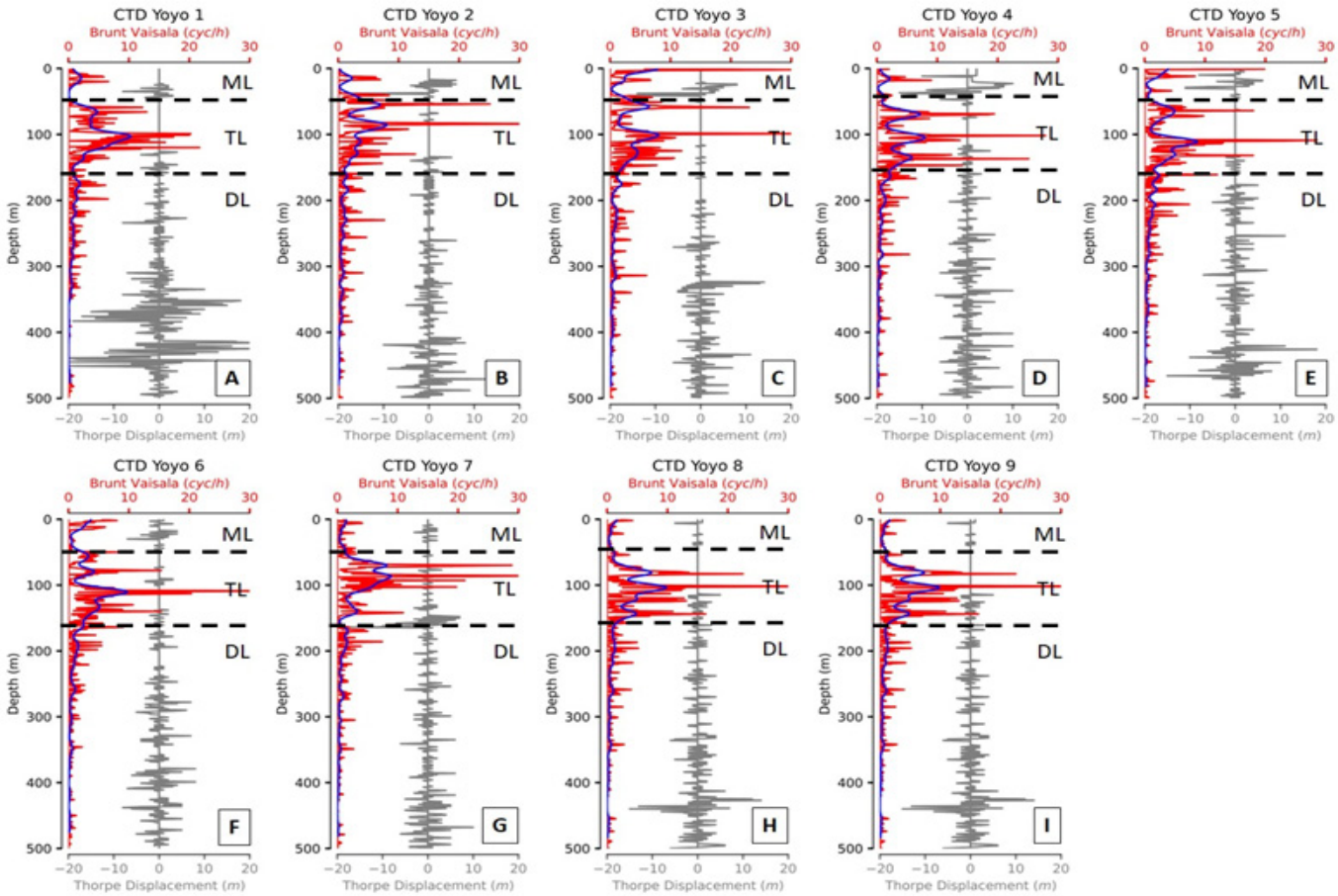

Figure 7. Vertical profiles of Brunt-Väisälä frequency (red) and thorpe displacement (gray) for replicates (A) CTD Yoyo 1, (B) CTD Yoyo 2, (C) CTD Yoyo 3, (D) CTD Yoyo 4, (E) CTD Yoyo 5, (F) CTD Yoyo 6, (G) CTD Yoyo 7, (H) CTD Yoyo 8, (I) CTD Yoyo 9, respectively. ML, TL, and DL are mixed layer, thermocline layer, and deep layer, respectively.

thermocline layer is the most stable layer compared to other layers, both in the mixed layer and the deep layer. The high level of stability is characterized by high values of Brunt-Väisälä and low values of thorpe displacement.

In all replications, the Brunt-Väisälä frequency ranged from 9.75E-09 to 3.54E-03 cycles per hour (cycles/hr) and the Thorpe shift ranged from -22 to 22 meters (m). We analyzed these data by depth layer for the study area in the Flores Sea as follows: Mixed Layer: Brunt-Väisälä frequency ranged from 1.41E-07 to 9E-04 cycles/hr, with an average of 1.1E-04 cycles/hr. The Thorpe shift ranged from -20 to 10 m. Thermocline Layer: Brunt-Väisälä frequency ranged from 1.35E-06 to 3.54E-03 cycles/hr, with an average of 3.39E-04 cycles/hr. The Thorpe shift ranged from -17 to 7 m. Deep Layer: The Brunt-Väisälä frequency ranges from 9.75E-09 to 7.64E-04 cycles/hour, with an average of 4.66E-05 cycles/hour. The Thorpe displacement ranges from -22 to 22 m.

This range reflects the vertical stability structure of the water mass, indicating that stability varies significantly with depth, which affects the mixing and stratification processes of the water column. The vertical stability structure of the water mass in the Flores Sea shows that the thermocline layer is the most stable layer based on the results obtained. The vertical structure of water mass stability is related to the vertical structure of turbulence that contributes to parameterization in mixing. At mixing points with strong turbulence, the formulation requires an understanding of physical processes (St. Laurent *et al.*, 2002).

The distribution of energy dissipation rate and vertical diffusivity values with depth at the study site is shown in Figure 8. Based on the estimation of indirect mixing using Thorpe's method, the energy dissipation value ranged from 1.02E-11 - 7.55E-06 W Kg^{-1} and vertical diffusivity ranged from 3.03E-07 - 2.16E-03 m^2 s^{-1}. The largest range of energy dissipation values is observed around the surface and the highest in the upper thermocline layer and decreases with depth. In general, the range of vertical diffusivity values shows the same trend. The range of energy dissipation and vertical diffusivity values is quite wide and begins to

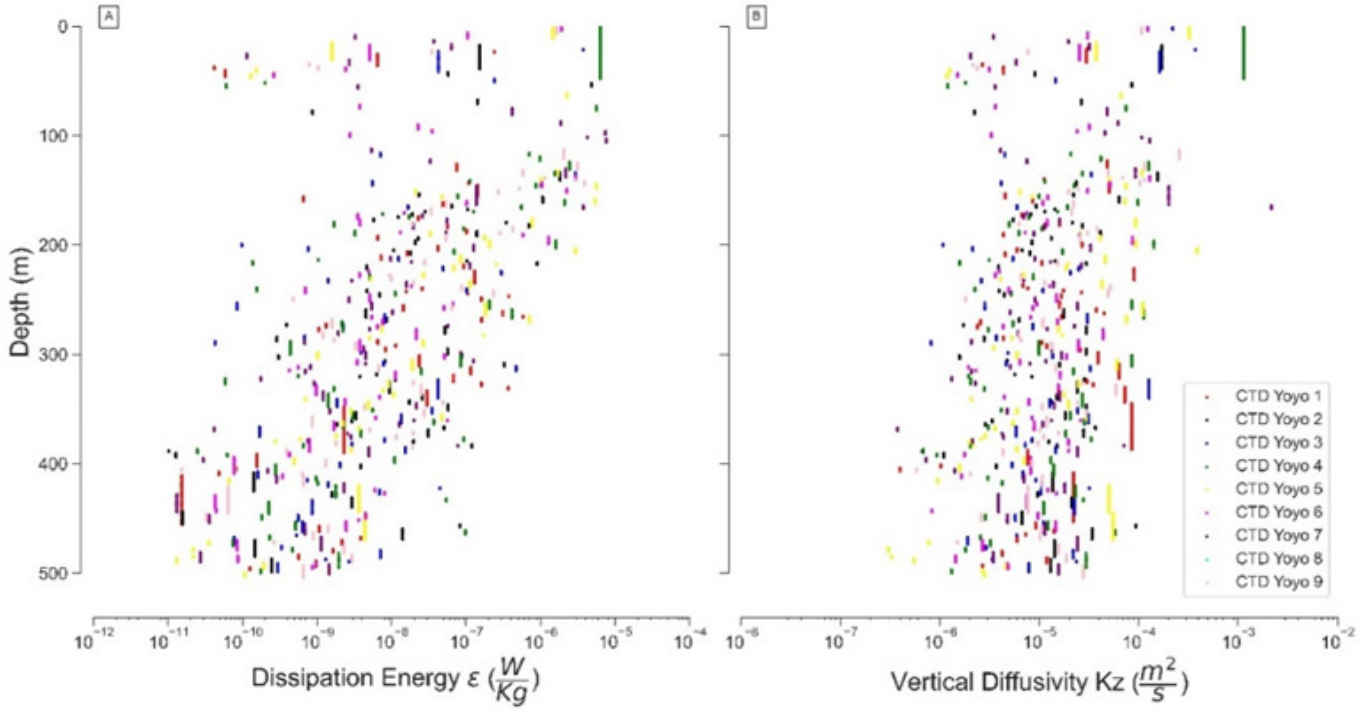

Figure 8. Vertical distribution of (A) Energy dissipation (ε) and (B) Vertical diffusivity (Kz) in CTD Yoyo replicates 1 - 9. The color description of CTD Yoyo replicates applies to (A) and (B).

narrow when entering the deep layer. The same pattern is observed by Cuypers *et al.* (2017) that higher energy dissipation values are observed in the thermocline layer. This could be due to the refraction effect of internal tidal energy stratification (Purwandana and Iskandar, 2020).

3.2 Discussion

3.2.1 Physical dynamics of waters

The dynamics of Indonesian waters are strongly influenced by various physical factors originating from both oceanic and atmospheric systems. The interaction between tidal forces, seasonal wind patterns, and air pressure distribution shapes complex ocean circulation patterns and affects the transport and mixing of water masses. Understanding these physical dynamics is essential for explaining hydro-oceanographic variability in tropical maritime regions such as Indonesia. Semidiurnal tides from the Pacific and Indian Oceans (Roberton and Fields, 2005) propagate through the Eastern Indonesian Waters with M2 as the main component controlling the tidal propagation. The existence of these tides contributes to the transport and mixing of water masses in Indonesian Waters which in turn plays an important role in regional current flow and global circulations (Roberton and Fields, 2008). Air pressure and temperature rely on the differences in energy received by the earth's surface and the wind blows from high to low pressure areas (differences in air pressure) (Nontji, 2005). The Indonesian region is strongly influenced by the Australia-Indonesia Monsoon (AIM), which is part of the global monsoon system in the southern hemisphere (Wang *et al.*, 2014).

The Indonesian region is seasonally influenced by 4 monsoons, namely for December-January-February (DJF), well-known as the northeast monsoon, March-April-May (MAM) as the first transitional monsoon, June-August (JJA) as the southwest monsoon, and September-October-November (SON) as the second transitional monsoon (Aldrian and Susanto, 2003). Trade winds push water from the tropical Pacific Ocean westward, causing higher sea levels and thus forming a pressure gradient between the Pacific and Indian Oceans (Wyrtki, 1987). The slowest surface winds occur during the transitional period (April and November). During the peak of the West and East monsoons, the surface wind speed reaches its peak, resulting in higher mixing in the upper layer (Nababan *et al.*, 2016). ITF water masses in the Flores Sea derive from the western and eastern passes of the Lifamatola Strait (Gordon *et al.*, 2010). The western ITF branches out into the Flores Sea and partly into the Lombok Strait and the remnant circulates into the Bali Sea and then into the Flores Sea (Atmadipoera and Hasanah, 2017).

3.2.2 Characteristics of turbulent mixing parameters

The histograms of energy dissipation and ver-

tical diffusivity of different layers (mixed, thermocline and deep) are shown in (Figure 9). The rate of energy dissipation and vertical diffusivity values with 1 m depth data interval as individual counts. Each layer has its own count range to highlight for clarity, as each layer consists of different amounts of data. Based on the amount of assessed data, most data were found in the deep layer, then the thermocline layer and the remnant were found in the mixed layer. In the mixed layer (surface), the energy dissipation rate is distributed fairly evenly, ranging from 1E-11 to 1E-05 W/kg, with no dominant peak observed (Figure 9A). While the vertical diffusivity values are in a fairly wide range ranging from 1E-06 to 5E-03 m2 s-1 (Figure 9D). In the thermocline layer, the energy dissipation rate ranges from 1E-11 to 1E-05 W Kg-1 with two peaks at 5E-08 W Kg-1 and 5E-06 W Kg-1 (Figure 9B). Meanwhile, the vertical diffusivity values range narrowly from 5E-05 to 5E-04 m²/s (Figure 9E). In the inner layer, the energy dissipation rate is evenly distributed from 1E-11 to 5E-05 W/kg, with a peak at 5E-08 W/kg (Figure 9C). Additionally, the vertical diffusivity values range narrowly from 5E-06 to 5E-04 m²/s, with a peak at 1E-05 m²/s (Figure 9F). The multi-modal distribution in the lower mixed layer and the uniform distribution in the surface layer indicate turbulence mixing driven by multiple forces (Mao *et al.*, 2022).

Next, we look at the layer values with an average per 50 m to make it clearer. The mean and standard deviation values of energy dissipation and vertical diffusivity were obtained (Figure 10). The near-surface layer has a relatively small value, then increases in the thermocline layer and then decreases again in the deep layer. The presence of strong vertical shear friction from the presence of ITF flow is strongly suspected to be a factor in increasing the value of the energy dissipation rate in the thermocline layer (Nagai and Hibiya, 2020). The energy dissipation value obtained at the research location is around 3.36E-07 W Kg-1 and the vertical diffusivity value is around 5.25E-05 m2 s-1. Based on the energy dissipation value of the observations that have been made, it is qualitatively quite consistent with the estimates made by Purwandana *et al.* (2020) using the CTD historical data set on the spatial distribution of energy dissipation in Indonesian waters. The value of the energy dissipation rate estimated at the research site has a smaller value than other studies at narrow locations as a mixing hotspot reaching O (Order) of 1E-02 W Kg-1 (Nagai and Hibiya, 2015). While in general, the value of vertical diffusivity is qualitatively close to the research of Ffield and Gordon (1992), obtaining a value of ~ 1E-04 m2 s-1 estimated using the advection-diffusion model in Indonesian waters.

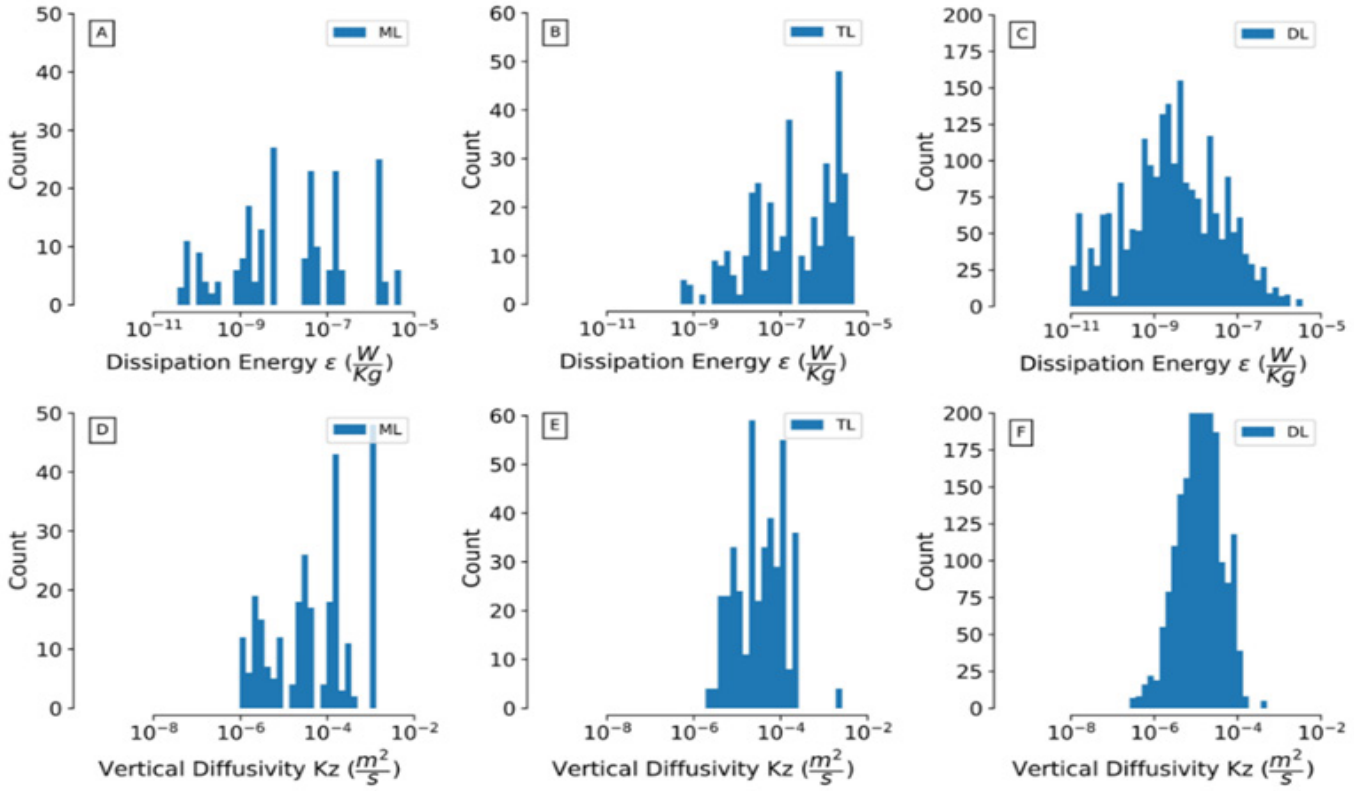

Figure 9. Statistical calculation of energy dissipation in (A) Mixed layer (ML), (B) Thermocline layer (TL), (C) Deep layer (DL) and vertical diffusivity in (D) Mixed layer (ML), (E) Thermocline layer (TL), (F) Deep layer (DL).

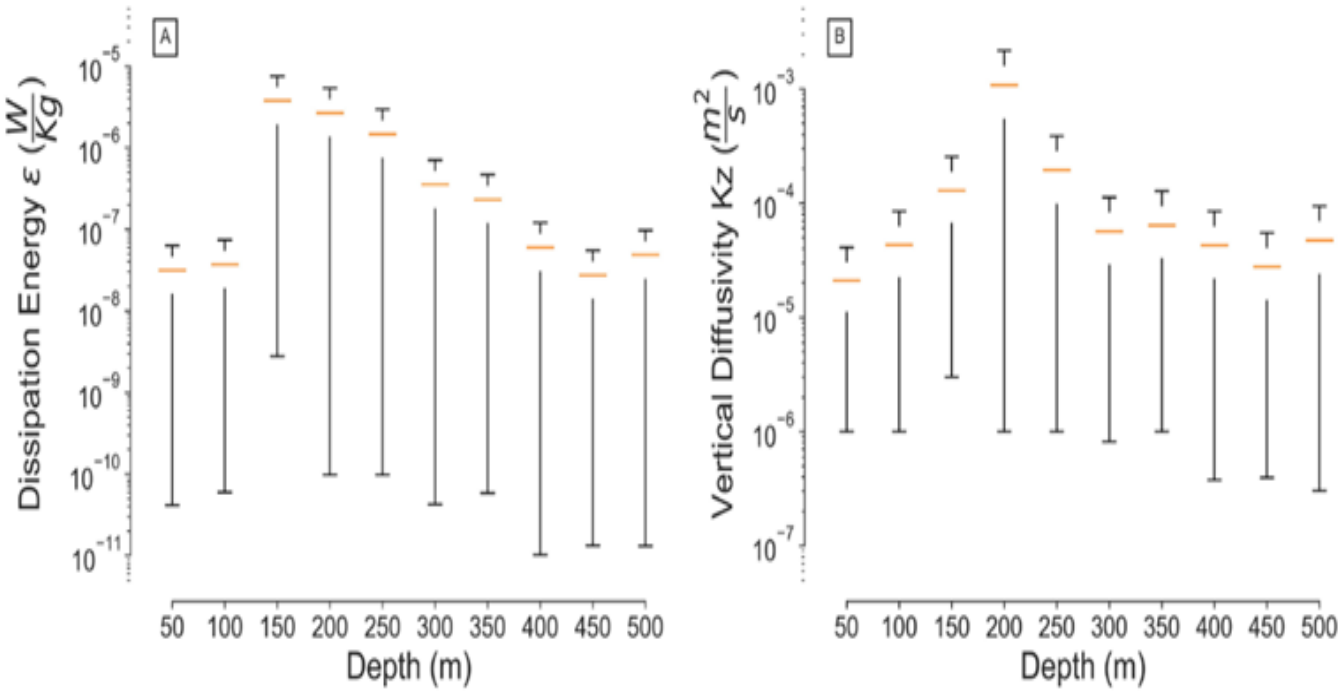

Figure 10. Mean values and standard deviations of all CTD data with averaging every 50 m (A) Energy dissipation and (B) Vertical diffusivity.

4. Conclusion

We investigated the water mass analysis and indirect estimation of turbulent mixing in the Flores Sea based on the acquisition of CTD instruments using the Yoyo casting method from 26 to 27 April 2023 for 9 replicates. We found four types of water masses, i.e., Java Sea water mass (JSW), JSW-NPIW, North Pacific Intermediate Water (NPIW) and (North Pacific Subtropical Water) NPSW. The Brunt-Väisälä frequency ranges from 9.75E-09 to 3.54E-03 cyc/h with the largest value in the thermocline layer. Higher values imply greater stability, indicating stratification and limited vertical movement of water masses. while the thorpe displacement ranges from -22 to 22 m with the smallest range in the thermocline layer. Positive displacements indicate the reversal and mixing of the water field, while negative values indicate the deposition of denser water. In addition, the mixed layer and the deep layer have small Brunt-Väisälä values and large thorpe displacement ranges. The energy dissipation value obtained from indirect measurements using Thorpe's method at the study site is around 3.36E-07 W Kg^{-1} and the vertical diffusivity value is around 5.25E-05 m^2 s^{-1}. The thermocline layer is stable with a large energy dissipation value which is strongly associated with the friction of the ITF. While the study sheds light on the correlation between the thermocline layer and energy dissipation-vertical diffusivity linked to the Indonesian Throughflow (ITF) in the Flores Sea, it has limitations. Relying solely on observational data may introduce uncertainties due to measurement variations, and the analysis overlooks potential contributors to turbulent mixing. Future research should consider incorporating diverse observational techniques, like numerical modeling and satellite remote sensing, to offer a more comprehensive understanding. Additionally, exploring the impact of turbulent mixing on marine ecosystems and climate dynamics would enhance practical relevance. Addressing these limitations would strengthen assessments of oceanic dynamics in the Flores Sea, benefiting both scientific understanding and practical applications.

Acknowledgement

We would like to thank the Indonesian Navy Hydrography and Oceanography Center (PUSHIDROSAL) for organizing the Jala Citra Expedition 3 - 2023 "Flores". In this research, data acquisition and preprocessing were fully supported by KRI Spica-934 as the research vehicle. We thank Lieutenant Colonel (P) Deirus Rizki Khair as the ship commander and task force commander along with the entire ship crew and researchers who were on board during data collection. We also thank the Geospatial Information Agency (BIG), European Center for Medium-Range Weather Forecasts (ECMWF) reanalysis 5 (ERA-5) climate Copernicus and ARMOR3D marine Copernicus for providing the data.

Authors' Contribution

The contributions of each author were as follows: GH and AYY conceived the study and designed the research framework. GH, AYY, and BP performed data analysis, while GH, AYY, and BP drafted the manuscript. AW and MC contributed to the interpretation of results and critical revision of the manuscript. All authors (GH, AYY, AW, BP, and MC) discussed the results and approved the final version of the manuscript.

Conflict of Interest

The authors declare that they have no competing interests.

Declaration of Artificial Intelligence (AI)

The author(s) affirm that no artificial intelligence (AI) tools, services, or technologies were employed in the creation, editing, or refinement of this manuscript. All content presented is the result of the independent intellectual efforts of the author(s), ensuring originality and integrity.

Funding Information

This research was generously funded by the Hydro-Oceanography Center, Indonesian Navy within the framework of Jala Citra 3 "Flores" 2023 Expedition.

References

Aldrian, E., & Susanto, R. D. (2003). Identification of three dominant rainfall regions within Indonesia and their relationship to sea surface temperature. *International Journal of Climatology: A Journal of the Royal Meteorological Society*, 23(12):1435-1452.

Arthur, R. S., Venayagamoorthy, S. K., Koseff, J. R., & Fringer, O. B. (2017). How we compute N matters to estimates of mixing in stratified flows. *Journal of Fluid Mechanics*, 831(2):1-10.

Atmadipoera, A. S., & Hasanah, P. (2017). Characteristics and variability of arlindo Flores and its coherence with the South Java coastal current. *Jurnal Ilmu dan Teknologi Kelautan Tropis*, 9(2):537-556.

Atmadipoera, A., Molcard, R., Madec, G., Wijffels, S., Sprintall, J., Koch-Larrouy, A., Jaya, I., & Supangat, A. (2009). Characteristics and variability of the Indonesian throughflow water at the outflow straits. *Deep Sea Research Part I: Oceanographic Research Papers*, 56(11):1942-1954.

Atmadipoera, A. S., & Widyastuti, P. (2014). A numerical modeling study on upwelling mechanism in Southern Makassar Strait. *Jurnal Ilmu dan Teknologi Kelautan Tropis*, 6(2):355-371.

Atmaja, R. R. P., Radjawane, I. M., & Tarya, A. (2019). Tidal current patterns in Wakatobi waters. Paper presented at Seminakel, University of Hang Tuah.

Caulfield, C., P. (2021). Layering, instabilities, and mixing in turbulent stratified flows. *Annual Review of Fluid Mechanics*, 53(5):113-145.

Cuypers, Y., Pous, S., Sprintall, J., Atmadipoera, A., Madec, G., & Molcard, R. (2017). Deep circulation driven by strong vertical mixing in the Timor basin. *Ocean Dynamics*, 67(2):191-209.

Dillon, T. M. (1982). Vertical overturns: A comparison of Thorpe and Ozmidov length scales. *Journal of Geophysical Research: Oceans*, 87(12):9601-9613.

Du, Y., & Qu, T. (2010). Three inflow pathways of the Indonesian throughflow as seen from the simple ocean data assimilation. *Dynamics of Atmospheres and Oceans*, 50(2):233-256.

Emery, W. J. (2001). Water types and water masses. *Encyclopedia of Ocean Sciences*, 6(1):3179-3187.

Fan, W., Jian, Z., Dang, H., Wang, Y., Bassinot, F., Han, X., & Bian, Y. (2018). Variability of the Indonesian throughflow in the Makassar strait over the last 30 Ka. *Scientific Reports*, 8(1):1-8.

Ferron, B., Mercier, H., Speer, K., Gargett, A., & Polzin, K. (1998). Mixing in the Romanche Fracture Zone. *Journal of Physical Oceanography*, 28(10):1929-1945.

Ffield, A., & Gordon, A. L. (1992). Vertical mixing in the Indonesian thermocline. *Journal of Physical Oceanography*, 22(1):184-195.

Fox-Kemper, B., Adcroft, A., Böning, C. W., Chassignet, E. P., Curchitser, E., & Danabasoglu, G. (2019). Challenges and prospects in ocean circulation models. *Frontiers in Marine Science*, 65(6):1-29.

Gordon, A., Sprintall, J., van Aken, H., Susanto, R. D., Wijffels, S., Molcard, R., Ffield, A., & Pranowo, W. (2010). The Indonesian throughflow during 2004-2006 as observed by the instant program. *Dynamics of Atmospheres and Oceans*, 50(2):113-114.

Gregg, M. C., D'Asaro, E. A., Riley, J. J., & Kunze, E. (2018). Mixing efficiency in the ocean. *Annual Review of Marine Science*, 10(1):443-473.

Guinehut, S., Dhomps, A.-L, Larnicol, G., & Le Traon, P.-Y. (2012). High resolution 3-D temperature and salinity fields derived from in situ and satellite observations. *Ocean Science*, 8(5):845-857.

Habibi, A., Setiawan, R. Y., & Zuhdy, A. Y. (2012). Wind-driven coastal upwelling along south of Sulawesi Island. *Ilmu Kelautan: Indonesian Journal of Marine Sciences*, 15(2):113-118.

Hao, J., Chen, Y., Wang, F., & Lin, P. (2012). Seasonal thermocline in the China Seas and Northwestern Pacific Ocean. *Journal of Geophysical Research: Oceans*, 117(2):1-14.

Harsono, G., Purwanto, B., Gultom, R. A., Puliwarna, T., Setiyadi, J., Ando, K., & Cobral, M. (2021). Seawater masses characteristics of the Bali Sea based on CTD Yoyo casting. *Ilmu Kelautan: Indonesian Journal of Marine Sciences*, 26(4):282-297.

Hersbach, H., Bell, B., Berrisford, P., Biavati, G., Horányi, A., Muñoz Sabater, J., Nicolas, J., Peubey, C., Radu, R., Rozum, I., Schepers, D., Simmons, A., Soci, C., Dee, D., & Thépaut, J. N. (2023). Era5 hourly data on single levels from 1940 to present. Copernicus climate change service (C3S) climate data store (CDS).

Jackett, D. J., & McDougall, T. J. (1995). Minimal adjustment of hydrographic profiles to achieve static stability. *Journal of Atmospheric and Oceanic Technology*, 12(2):381-389.

Karang, I. W. G. A., Chonnaniyah, & Osawa, T. (2019). Internal solitary wave observations in the Flores Sea using the himawari-8 geostationary satellite. *International Journal of Remote Sensing*, 41(15):5726-5742.

Koch-Larrouy, A., Lengaigne, M., Terray, P., Madec, G., & Masson, S. (2010). Tidal mixing in the Indonesian seas and its effect on the tropical climate system. *Climate Dynamics*, 34(1):891-904.

Kunarso, Situmorang, R. P., Wulandari, S. Y., & Ismanto, A. (2018). Variability of upwelling in Bone Bay and Flores Sea. *International Journal of Civil Engineering and Technology*, 9(10):742-751.

Kurniawan, R., Suriamihardja, Dadang., & Muhammad, A. (2018). Upwelling dynamic based on satellite and INDESO data in the Flores Sea. *Journal of Physics: Conference Series*, 979(1):1-12.

Liu, C., Huo, D., Liu, Z., Wang, X., Guan, C., Qi, J., & Wang, F. (2022). Turbulent mixing in the barrier layer of the equatorial Pacific Ocean. *Geophysical Research Letters*, 49(5):1-9.

Liu, C., Köhl, A., Liu, & Z. Stammer D. (2016). Deep-reaching thermocline mixing in the equatorial Pacific cold tongue. *Nature Communications*, 7(1):1-15.

Mao, H., Feng, M., Qi, Y., & Keesing, J. K. (2022). Observation of strong turbulent mixing in the Australian North West shelf. *Regional Studies in Marine Science*, 55(1):1-15.

McDougall, T. J. & Barker, P. M. (2011). Getting started with TEOS10 and the Gibbs Seawater (GSW) oceanographic toolbox. SCOR/IAPSO WG127. 28 pp. ISBN 978-0-646-55621-5.

Mulet, S., Rio, M. H., Mignot, A., Guinehut, S., & Morrow, R. (2012). A new estimate of the global 3-D geostrophic ocean circulation based on satellite data and in-situ measurements. *Deep Sea Research Part II: Topical Studies in Oceanography*, 4(12):77-80.

Nababan, B., Rosyadi, N., Manurung, D., Natih, N. M., & Hakim, R. (2016). The seasonal variability of sea surface temperature and chlorophyll-a concentration in the South of Makassar Strait. *Procedia Environmental Sciences*, 33(2016):583-599.

Nagai, T., & Hibiya, T. (2015). Internal tides and associated vertical mixing in the Indonesian archipelago. *Journal of Geophysical Research*, 120(1):3373-3390.

Nagai, T., & Hibiya, T. (2020). Combined effects of tidal mixing in narrow straits and the Ekman transport on the sea surface temperature cooling in the southern Indonesian Seas. *Journal of Geophysical Research*, 125(1):1-13.

Nagai, T., Hibiya, T., & Syamsudin, F. (2021). Direct estimates of turbulent mixing in the Indonesian archipelago and its role in the transformation of the Indonesian throughflow waters.

Geophysical Research Letters, 48(1):1-9.

Napitupulu G., Nurdjaman, S., Fekranie, N. A., Suprijo, S., & Subehi, L. (2022). Analysis of upwelling in the Southern Makassar Strait in 2015 using aqua-modis satellite image. *Journal of Water Resources and Ocean Science*, 11(4):64-70.

Nontji, A. (2005). Archipelago Sea. Anugerah Nontji. Jakarta: Djambatan. Thurman.

Osborn, T. R. (1980). Estimates of the local rate of vertical diffusion from dissipation measurements. *Journal of Physical Oceanography*, 10(1):83-89.

Putriani, P. Y., Atmadipoera, A. S., & Nugroho, D. (2019). Interannual variability of Indonesian throughflow in the Flores Sea. *IOP Conference Series*: *Earth and Environmental Science*, 278(1):1-14.

Purwandana, A., Cuypers, Y., Bouruet-Aubertot, P., Nagai, T., Hibiya, T., & Atmadipoera, A. S. (2020). Spatial structure of turbulent mixing inferred from historical CTD datasets in the Indonesian Seas. *Progress in Oceanography*, 184(5):1-20.

Purwandana, A., & Iskandar, M. R. (2020). Turbulent mixing inferred from CTD datasets in the Western Tropical Pacific Ocean. *Ilmu Kelautan*: *Indonesian Journal of Marine Sciences*, 25(4):148-156.

Putri, A. R. S., Zainuddin, M., Musbir., Mustapha, M. A., Hidayat, R., & Putri, R. S. (2021). Impact of increasing sea surface temperature on skipjack tuna habitat in the Flores Sea, Indonesia. *IOP Conference Series*: *Earth and Environmental Science*, 763(1):1-9.

Ray, R. D., Egbert, G. D., & Erofeeva, S. Y. (2005). A brief overview of tides in the Indonesian Seas. *Oceanography*, 18(4):74-79.

Ray, R. D., & Susanto, R. D. (2016). Tidal mixing signatures in the Indonesian Seas from high-resolution sea surface temperature data. *Geophysical Research Letters*, 43(8):1-9.

Robertson, R., & Ffield, A. (2005). M2 baroclinic tides in the Indonesian Seas. *Oceanography*, 18(4):62-73.

Robertson, R., & Ffield, A. (2008). Baroclinic tides in the Indonesian Seas: Tidal fields and comparisons to observations. *Journal of Geophysical Research*: *Oceans*, 113(7):1-22.

Sharples, J., Moore, C. M., & Abraham, E. R. (2001). Internal tide dissipation, mixing, and vertical nitrate flux at the shelf edge of NE New Zealand. *Journal of Geophysical Research*: *Oceans*, 106(7):14069-14081.

Silaban, L. L., Atmadipoera, A. S., Hartanto, M. T., & Herlisman. (2021). Water mass characteristics in the Makassar Strait and Flores Sea in August-September 2015. *IOP Conf. Series*: *Earth and Environmental Science*, 944(2021):1-12.

Sprintall, J., Gordon, A. L., Lee, T., Potemra, J. T., Pujiana, K., & Wijffels, S. E. (2014). The Indonesian Seas and their role in the Couple Ocean-Climate System. *Nature Geoscience*, (7):487-492.

Sprintall, J., Gordon, A. L., Wijffels, S. E., Feng, M., Hu, S., Koch-Larrouy, A., Phillips, H., Nugroho, D., Napitu, A., & Pujiana, K. (2019). Detecting change in Indonesian Seas. *Frontiers in Marine Science*, 247(6):1-24.

Sprintall, J., Wijffels, S., Gordon, A. L., Ffield, A., Molcard, R., Susanto, R. D., Soesilo, I., Sopaheluwakan, J., Surachman, Y., & van Aken, H. M. (2004). A new international array to measure the Indonesian throughflow: INSTANT. *EOS, Transactions American Geophysical Union*, 85(39):369-376.

Sprintall, J., Wijffels, S. E., Molcard, R., & Jaya, I. (2009). Direct estimates of the Indonesian throughflow entering the Indian Ocean: 2004-2006. *Journal of Geophysical Research*, 114(1):1-19.

St. Laurent, L. C., Simmons, H. L., & Jayne, S. R., (2002). Estimating tidally driven mixing in the deep ocean. *Geophysical Research Letters*, 29(23):1-21.

Susanto, R. D., Ffield, A., Gordon, A. L., & Adi, T. R. (2012). Variability of Indonesian throughflow within Makassar Strait: 2004-2009. *Journal of Geophysical Research*, 117(9):1-16.

Susanto, R. D., & Song, Y. T. (2015). Indonesian throughflow proxy from satellite altimeters and gravimeters. *Journal of Geophysical Research*, 120(4):1-12.

Thorpe, S. A. (1977). Turbulence and mixing in a Scottish Loch. *Philosophical Transactions of the Royal Society of London Series A*, 286(1):125-181.

Wang, P. X., Wang, B., Cheng, H., Fasullo, J., Guo, Z. T., Kiefer, T., & Liu, Z. Y. (2014). The global monsoon across timescales: Coherent vari-

ability of regional monsoons. *Climate of the Past*, 10(6):2007-2052.

Wei, Z. X., Fang, G. H., Susanto, R. D., Adi, T. R., Fan, B., Setiawan, A., Li, S., Wang, Y. G., & Gao, X. M. (2016). Tidal elevation, current, and energy flux in the area between the South China Sea and Java Sea. *Ocean Science*, 12(2):517-531.

Wunsch, C., & Ferrari, R. (2004). Vertical mixing, energy, and the general circulation of the oceans. *Annual Review of Fluid Mechanics*, 36(1):281-314.

Wyrtki, K. (1987). Indonesian through flow and the associated pressure gradient. *Journal of Geo physical Research*, 92(12):12941-12946.

Wyrtki, K. (1961). Physical oceanography of the Southeast Asian Waters. United States of America: The University of California, p.220.

Yang, Q., Zhao, W., Li, M., & Tian, J. (2014). Spatial structure of turbulent mixing in the Northwestern Pacific Ocean. *Journal of Physical Oceanography*, 44(8):2235-2247.

Yuliardi, A. Y., Atmadipoera, A. S., Harsono, G., N. Natih, N. M., & Ando, K. (2021). Analysis of characteristics and turbulent mixing of seawater mass in Lombok Strait. *Ilmu Kelautan*: *Indonesian Journal of Marine Sciences*, 26(2):95-109.